ELSEVIER

Journal of Nuclear Materials 307–311 (2002) 212–216

journal of nuclear materials

www.elsevier.com/locate/jnucmat

# Recent results for the ferritics isotopic tailoring (FIST) experiment

D.S. Gelles [a,*,1], M.L. Hamilton [a], B.M. Oliver [a], L.R. Greenwood [a], S. Ohnuki [b], K. Shiba [c], Y. Kohno [d], A. Kohyama [e], J.P. Robertson [f]

[a] *Pacific Northwest National Laboratory, MS P8-15, P.O. Box 999, Richland, WA 99352, USA*
[b] *University of Hokkaido, Sapporo 060-0808, Japan*
[c] *JAERI Tokai, Ibaraki-ken 319-1195, Japan*
[d] *Muroran Institute of Technology, 27-1 Mizamoto-cho, Muroran 050-8585, Japan*
[e] *Kyoto University, Kyoto, Japan*
[f] *Oak Ridge National Laboratory, Oak Ridge, TN 37831, USA*

**Abstract**

An alloy of F82H prepared using the isotope $^{54}$Fe in order to encourage H and He production in a fission reactor has been irradiated in the HFIR JP20 experiment at three temperatures to 7 dpa as TEM disks. Irradiated disks were shear punch tested, examined by TEM, analyzed for He and H content, and compared with previous results in order to quantify irradiation hardening due to transmutation-induced H and He. Hardening due to irradiation is found following irradiation at 300 and 400 °C, that is intermediate between that at lower and higher dose, but hardening is negligible following irradiation at 500 °C. Microstructural examinations show typical behavior of irradiation as a function of irradiation temperature, with moderate swelling after 400 °C irradiation but few bubbles after irradiation at 300 °C. Correlations of change in hardening with He and H content show little indication of transmutation-induced hardening, but measured H levels do not agree with predictions and therefore H production and analysis requires further study.


## 1. Introduction

The production of transmutation-induced gases such as H and He remains a key concern regarding use of martensitic steels for first wall applications in a fusion reactor. Data exists that indicates both H and He can cause significant embrittlement. In an effort to understand this behavior, an alloy of F82H has been prepared using the isotope $^{54}$Fe in order to encourage H and He production in a fission reactor. Post-irradiation deformation response, microstructural change, and transmutation induced gas generation of hydrogen and helium has been reported based on measurements of two HFIR irradiated specimen conditions of this isotopically tailored alloy in order to study hydrogen and helium embrittlement in single variable experiments [1,2]. Those results were shown to indicate that transmutation-induced hydrogen may play an important role in irradiation embrittlement [3]. Recently, three more isotopically tailored specimen conditions irradiated in HFIR to ~8 dpa at 300, 400 and 500 °C were made available for examination. This report is intended to provide post-irradiation deformation response based on the shear punch technique, microstructural examination and transmutation-induced gas content for these three conditions.

## 2. Experimental procedures

Two transmission electron microscopy (TEM) disks of $^{54}$Fe isotopically tailored F82H were obtained from

* Corresponding author. Tel.: +1-509 376 3141; fax: +1-509 376 0418.
*E-mail address:* ds_gelles@pnl.gov (D.S. Gelles).
[1] Pacific Northwest National Laboratory (PNNL) is operated by the US Department of Energy by Battelle Memorial Institute under contract DE-AC06-76RLO-1830.

0022-3115/02/$ - see front matter 
PII: S0022-3115(02)01181-9

each of the HFIR JP20 experiment positions 6, 9 and 7. The experimental design of the JP20 experiment is described in Ref. [4], specimen loading is documented in Ref. [5] and irradiation history and neutron dosimetry can be found in Ref. [6]. The corresponding specimen identification codes are: C601 and C602 for position 6 at 300 °C, C605 and C606 for position 9 at 400 °C, and C609 and C610 for position 7 at 500 °C. One disk for each condition was tested by shear punching and then prepared as a thin foil using the central 1 mm disk created during shear punch testing as described previously [1,2]. The outer ring that remained was then sectioned and used for hydrogen and helium analyses using procedures described previously [7].

## 3. Results

Results of shear punch testing are shown as test curves in Fig. 1. Tabulated results can be found in Ref. [8]. Fig. 1 includes results from previous tests. From these results, it can be shown that irradiation at 500 °C produces only slightly higher hardening than in the unirradiated condition whereas irradiation at 300 and 400 °C produces similar levels of hardening, intermediate between that due to irradiation at 250 °C to 2.4 dpa and irradiation at 300 °C to 34 dpa.

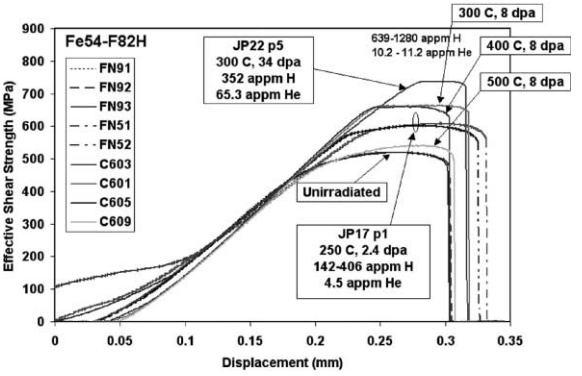


Fig. 1. Shear punch test traces for FIST specimens containing $^{54}$Fe.

Helium concentrations have been measured for specimens C601, C605 and C609 and the results are tabulated in Ref. [8] along with results from previous FIST measurements. Hydrogen concentrations were also measured and those results are tabulated in Ref. [8] along with previous results. Helium levels for the three conditions are found to be similar indicating that changes in irradiation temperature did not affect helium retention. Hydrogen levels varied with temperature, the highest levels found after irradiation at 400 °C, with lower hydrogen following irradiation at 300 °C and the lowest following irradiation at 500 °C.

Microstructural examinations have been performed on each of the conditions available. Examples of these microstructures at low magnification are provided in Fig. 2, with one example following irradiation at 300 °C, two examples following irradiation at 400 °C and one example following irradiation at 500 °C. All show typical martensite lath structure decorated with $M_{23}C_6$ carbide. Of particular note are the voids showing at low density following irradiation at 400 °C (and therefore two examples are given). Also, it is possible but difficult to quantify, that following irradiation at 500 °C precipitate decoration of lath boundaries is more complete.

The dislocation and bubble structures were studied in greater detail by examining these microstructures in dark field under dislocation contrast. Examples are provided in Fig. 3 comparing a region of interest for each condition under $g = 0\,1\,\bar{1}$ and $2\,0\,0$ dark field along with a bright field image, for C601 and C605 in void contrast and for C609 in dislocation contrast. Fig. 3 shows that the dislocation structure changes with irradiation temperature, size increasing and density decreasing with increasing temperature. However, other

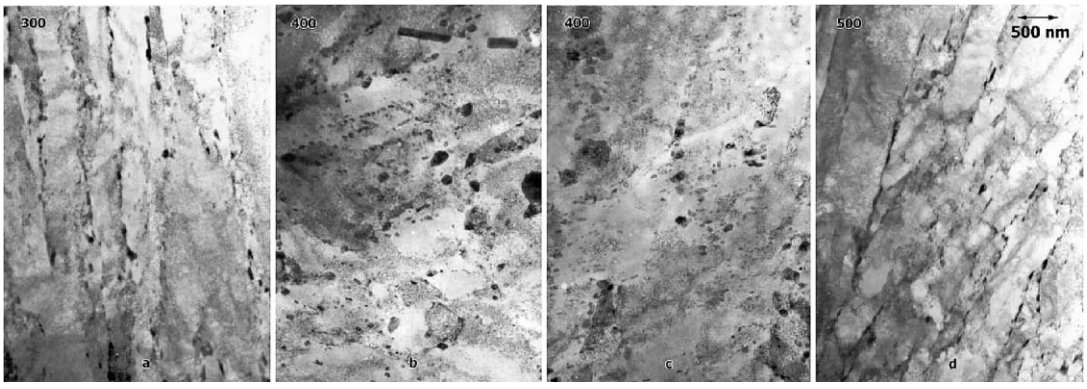


Fig. 2. Low magnification examples of microstructures in C601 (a), C605 (b) and (c), and C609 (d).

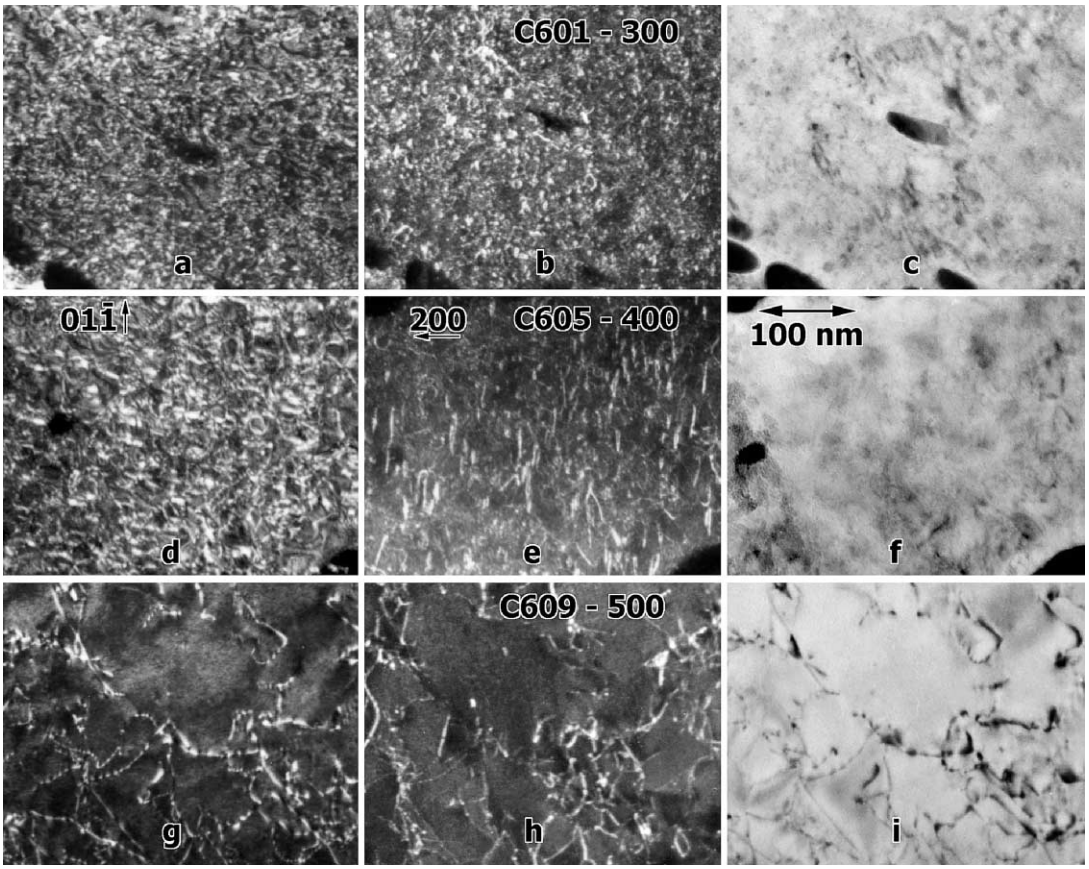


Fig. 3. Dislocation structure in conditions C601, C605 and C609 shown in $g = 01\bar{1}$, 200 and bright field contrast, respectively.

differences can be identified. For example, $a\langle 100\rangle$ Burgers vectors predominate following irradiation at 400 °C, but are not present following irradiation at 500 °C and may not be present following irradiation at 300 °C. This is demonstrated most straightforwardly in Fig. 3(e) where horizontal features (perpendicular to the operating 200 diffraction vector) are of Burgers vector $a[100]$ whereas all other dislocation line segments (in weaker contrast) are of type $(a/2)\langle 111\rangle$. Also of note are smaller equiaxed features in Fig. 3(a) and (b) about 5 nm in diameter. These may be small loops or gas bubbles, but because they are not visible in Fig. 3(c), it is expected that they are due to precipitation, possible $\alpha'$ or carbide. Finally, bubbles on the order of 5 nm in diameter may be seen in Fig. 3(c) but the density is apparently low.

## 4. Discussion

Irradiation hardening response is plotted as a function of dose and temperature for effective shear yield and maximum strength, respectively, in Fig. 4(a) through (d). Data from samples C601, C605 and C609 is labeled 300 °C, 400 °C and 500 °C, respectively. Behavior of strength as a function of dose in Fig. 4(a) and (c) follows expected behavior for 300 and 400 °C but strength following irradiation at 500 °C is much lower. This is further demonstrated in Fig. 4(b) and (d). Therefore, it is reasonable to directly compare response following irradiation at 250, 300 and 400 °C. Note that this response is typical of irradiation hardening without the influence of transmutation-induced gases.

In order to identify effects of He and H produced by transmutation during irradiation, it is best to plot hardening behavior as a function of He and H as shown previously [9]. Therefore, change in effective shear strength is shown plotted as a function of He and H content in Fig. 5. Fig. 5 includes previous results as well as results for conditions C601, C605 and C609. From Fig. 5, several conclusions can be drawn. The behavior found previously as a function of He is similar to that in [9, Fig. 8], except for results at 500 °C. Therefore, conclusions drawn previously may still apply: that it is possible that there is no effect of He on yield response whereas a bi-linear response can be identified for the

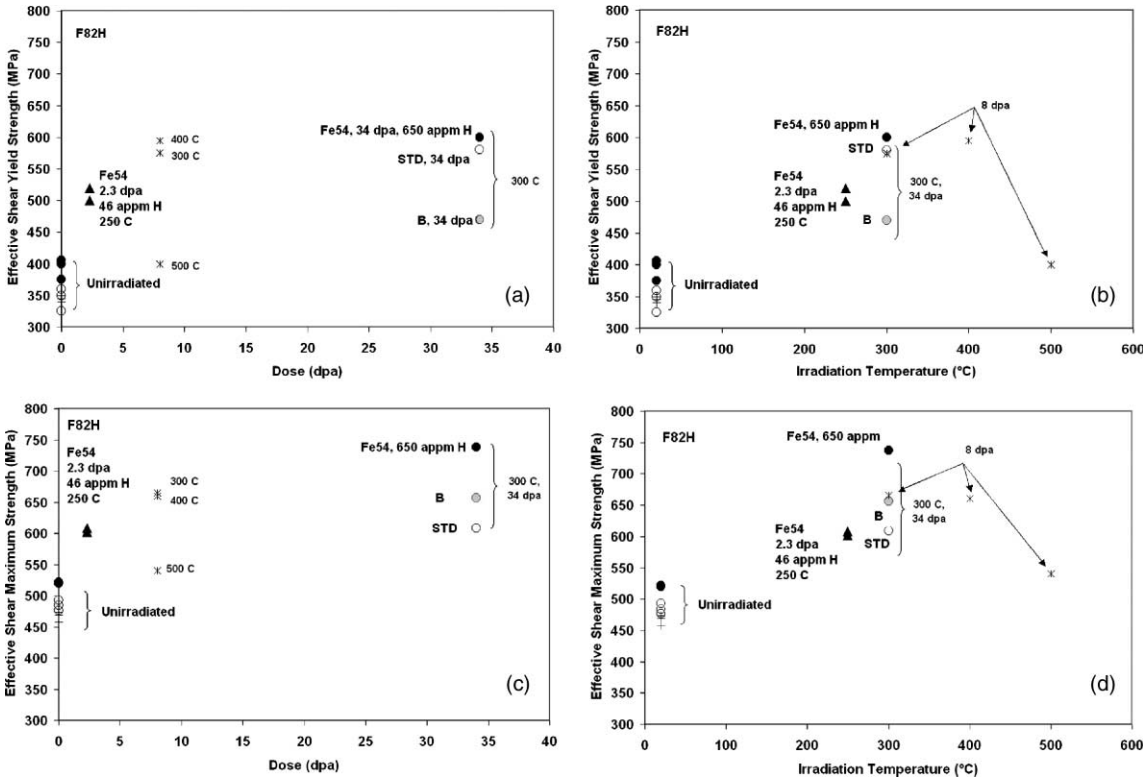


Fig. 4. Effective shear properties as a function of dose for isotopically tailored F82H.

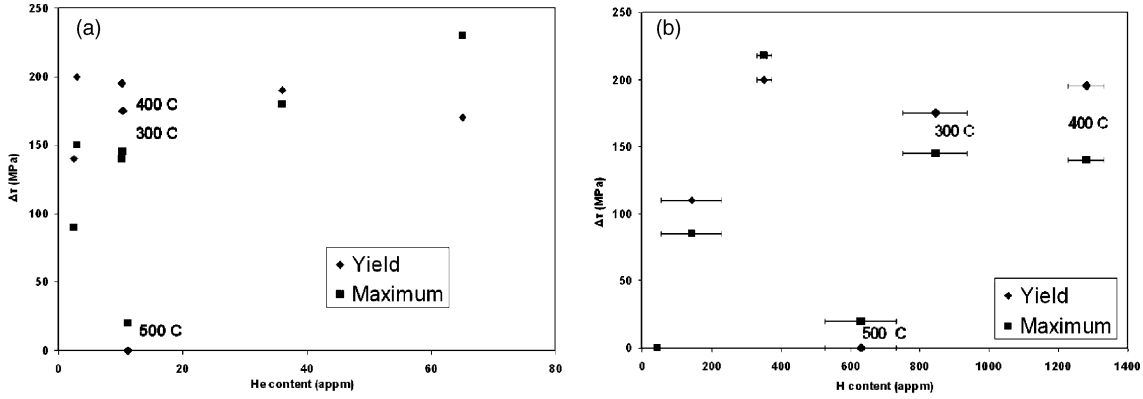


Fig. 5. Change in $\tau_{ys}$ and $\tau_{ms}$ due to irradiation as a function of (a) He content and (b) H content for FIST alloys.

maximum strength if one excludes results at 500 °C. Bilinear response is indicated because zero hardening is imposed for zero He. Results as a function of H must be interpreted differently. Data for C601, C605 and C609 give very different irradiation hardening behavior as a function of H compared to response found previously, with no straightforward correlation evident.

It must be noted that the measurements of helium in specimens C601, C605 and C609 fit predicted behavior whereas measurements for H are considerably higher than expected. This is demonstrated in Fig. 6(a) and (b) showing He and H measured levels in comparison with prediction. Note that He measurements agree with prediction whereas values measured for H are above prediction but earlier measurements for higher dose are considerably below prediction. The earlier data was interpreted to indicated that H can be lost during irradiation whereas the present data indicated that not only is

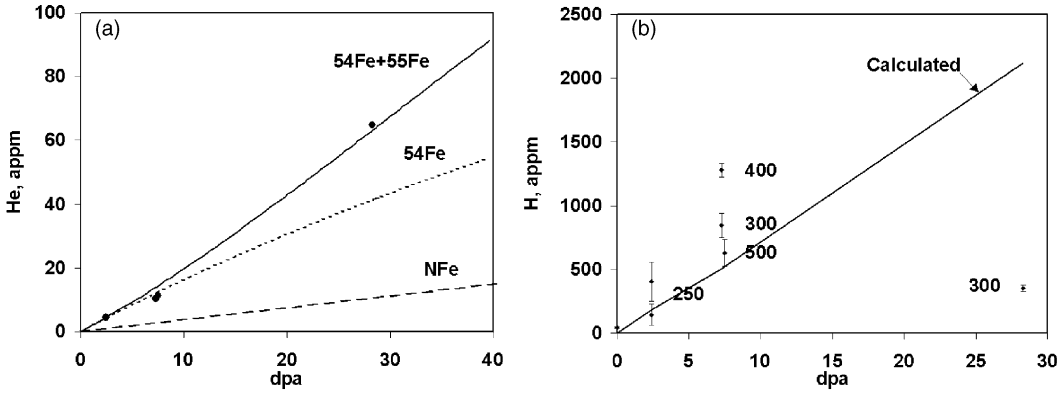


Fig. 6. Helium and hydrogen production in $^{54}$Fe isotopically tailored F82H, measurement versus prediction.

H not lost, it can be generated at higher than expected rates.

Only one of the two specimens available for examination has been used. Therefore, consideration is being given to using the remaining specimens for remeasurement of H. Also, this work would be enhanced greatly if control conditions (those without $^{54}$Fe) were available. Then it should be possible to objectively account for effects of transmutation-induced He and H. Unfortunately, it has not yet been possible to obtain such control conditions.

## 5. Conclusions

Three conditions of isotopically tailored F82H irradiated in the HFIR JP20 experiment have been tested, examined by TEM, and analyzed for He and H content in order to quantify irradiation hardening due to transmutation-induced helium and hydrogen.

Hardening due to irradiation is found following irradiation at 300 and 400 °C, that is intermediate between that at lower and higher dose, but hardening is negligible following irradiation at 500 °C.

Microstructural examinations show typical behavior of irradiation as a function of irradiation temperature, with moderate swelling after 400 °C irradiation but few bubbles after irradiation at 300 °C.

## References

[1] M.L. Hamilton, D.S. Gelles, S. Ohnuki, K. Shiba, Y. Kohno, A. Kohyama, DOE/ER-0313/25, 1999, p. 136.
[2] D.S. Gelles, S. Ohnuki, K. Shiba, Y. Kohno, A. Kohyama, J.P. Robertson, M.L. Hamilton, DOE/ER-0313/25, 1999, p. 143.
[3] S. Ohnuki, Y. Kohno, A. Kohyama, K. Shiba, D.S. Gelles, M.L. Hamilton, J.P. Robertson, ICFRM-9, Colorado Springs, October 1999, paper 7.04.
[4] J.E. Pawel, R.L. Senn, DOE/ER-0313/12, 1992, p. 15.
[5] J.E. Pawel, A.W. Longest, R.L. Senn, K. Shiba, D.W. Weatherly, R.G. Sitterson, DOE/ER-0313/15, 1994, p. 3.
[6] L.R. Greenwood, C.A. Baldwin, DOE/ER-0313/18, 1998, p. 305.
[7] L.R. Greenwood, B.M. Oliver, S. Ohnuki, K. Shiba, Y. Kohno, A. Kohyama, J.P. Robertson, J.W. Meadows, D.S. Gelles, J. Nucl. Mater. 283–287 (2000) 1438.
[8] D.S. Gelles, M.L. Hamilton, B.M. Oliver, L.R. Greenwood, S. Ohnuki, K. Shiba, Y. Kohno, A. Kohyama, J.P. Robertson, DOE/ER-0313/29, 2001, p. 93.
[9] D.S. Gelles, M.L. Hamilton, B.M. Oliver, L.R. Greenwood, DOE/ER-0313/27, 2000, p. 149.